



Published in final edited form as:

*Science*. 2015 April 3; 348(6230): 136–139. doi:10.1126/science.1258867.

## A shed NKG2D ligand that promotes natural killer cell activation and tumor rejection

Weiwen Deng<sup>1</sup>, Benjamin G. Gowen<sup>1</sup>, Li Zhang<sup>1</sup>, Lin Wang<sup>1</sup>, Stephanie Lau<sup>1</sup>, Alexandre Iannello<sup>1</sup>, Jianfeng Xu<sup>1</sup>, Tihana L. Rovis<sup>2</sup>, Na Xiong<sup>3</sup>, and David H. Raulet<sup>1,\*</sup>

<sup>1</sup>Department of Molecular and Cell Biology, and Cancer Research Laboratory, University of California at Berkeley, Berkeley, CA, 94720, USA

<sup>2</sup>Center for Proteomics University of Rijeka Faculty of Medicine Brace Branchetta 20, 51000 Rijeka, CROATIA

<sup>3</sup>Department of Veterinary and Biomedical Sciences, Pennsylvania State University, 115 Henning Bldg, University Park, PA 16802, USA

### Abstract

Immune cells, including natural killer (NK) cells, recognize transformed cells and eliminate them in a process termed immunosurveillance. It is thought that tumor cells evade immunosurveillance by shedding membrane ligands that bind to the NKG2D activating receptor on NK cells and/or T cells, and desensitize these cells. In contrast, we show that in mice, shedding of MULT1, a high affinity NKG2D ligand, causes NK cell activation and tumor rejection. Recombinant soluble MULT1 stimulated tumor rejection in mice. Soluble MULT1 functions, at least in part, by competitively reversing a global desensitization of NK cells imposed by engagement of membrane NKG2D ligands on tumor-associated cells, such as myeloid cells. The results overturn conventional wisdom that soluble ligands are inhibitory, and suggest a new approach for cancer immunotherapy.

---

NK cells and some T cells employ activating receptors such as NKG2D to recognize and eliminate infected and transformed cells that upregulate ligands for these receptors (1). There are 6–8 different NKG2D ligands, which are poorly expressed by normal cells but upregulated in cancer cells (2). Many tumor cells release soluble NKG2D ligands through proteolytic shedding, alternative splicing, or exosome secretion (2, 3). Numerous reports conclude that excreted NKG2D ligands modulate NKG2D from the cell surface and desensitize anti-tumor effector cells (4, 5), although a functional impact of soluble NKG2D ligands is not always observed (6–9). To study shed NKG2D ligands in a controlled setting, we focused on the mouse ligand MULT1, which is commonly upregulated in primary tumors

---

\*Correspondence: raulet@berkeley.edu, Tel: 510-642-9521, Fax: 510-642-1443.

#### Supplementary materials

Materials and Methods

Table S1

Fig. S1 to S14

Author contribution

References (29–32)

(10) and is a transmembrane protein like the human ligands MICA, MICB, ULBP4 and ULBP5 (11). Analysis of fibroblasts transduced with either N- or C-terminally tagged MULT1 revealed an N-terminal species (23 kD after deglycosylation) shed into the culture supernatant (fig. S1A), and a 24 kD membrane “stub” in the cell lysates, in addition to full length (around 42 kD) MULT1 (fig. S1B). Inhibiting matrix metalloproteinases blocked MULT1 shedding (fig. S1C).

HA-MULT1-transduced fibroblasts produced nearly 8-fold more shed MULT1 than untransduced fibroblasts (fig. S2). WEHI-7.1 and C1498 but not human 293T cell lines excreted MULT1 produced endogenously. We detected serum MULT1 (mean concentration ~250 ng/ml) in most tumor-bearing *Eμ-myc* transgenic mice, which frequently develop MULT1+ tumors (10), but not in most non-transgenic littermates (Fig. 1A). Very high concentrations of soluble MULT1 were also detected in sera of *ApoE*<sup>-/-</sup> mice fed a high fat diet (Fig. 1A). Given that atherosclerosis and liver inflammation in such mice are largely dependent on NKG2D function (12), it seemed unlikely that soluble MULT1 inhibits NKG2D function. Thus, MULT1 is released from cell lines that naturally or ectopically express MULT1, and accumulates in sera of animals with spontaneous tumors and NKG2D-dependent inflammatory disease.

Purified shed HA-MULT1 bound to NKG2D with high affinity (average  $K_D$  of 13 nM±3.8 nM) (fig. S3), similar to the affinity reported for recombinant MULT1 (13). In parallel, we engineered fibroblasts to secrete an ectodomain fragment of HA-MULT1 (which we call secMULT1). SecMULT1 also bound to NKG2D with high affinity (19 nM±4.3 nM) (fig. S3).

To test the function of soluble MULT1, we engineered two NKG2D ligand-negative B6 strain tumor cell lines to secrete secMULT1. Surprisingly, both cell lines were rejected by syngeneic B6 mice compared to cells transduced with empty vector (Fig. 1B, fig. S4A), despite the absence of cell surface MULT1 (fig. S4B). Tumor cells transduced with full-length MULT1 (mutated in the cytoplasmic tail to optimize cell surface expression (14), fig. S4B) were also rejected (Fig. 1B). B16-secMULT1 cells were still rejected in B6 hosts that had been depleted of CD8+ cells but grew progressively in B6 and *Rag1*<sup>-/-</sup> hosts that had been depleted of NK1.1+ cells (Fig. 1C, fig. S5). Hence, NK cells but not CD8+ cells participate in the rejection of B16-secMULT1. B16 cells with inducible secMULT1 (fig. S6) were also partially rejected (Fig. 1D). In this case, the secMULT1 lacked an epitope tag, showing that rejection occurs without a tag. A mixture of B16 (90%) and B16-secMULT1 (10%) cells was also rejected, demonstrating that sec-MULT1 acts extrinsically (Fig. 1E). These data ruled out the possibility that rejection was due solely to intrinsic stress responses in sec-MULT1 expressing tumor cells. Instead, the data suggested that secMULT1 mobilizes or activates anti-tumor effector cells.

To address whether tumor cells secreting secMULT1 activate NK cells, we adapted a short-term *in vivo* NK induction protocol (15, 16), by injecting irradiated tumor cells intraperitoneally in normal mice. Injection of B16-secMULT1 or B16 cells induced similar modest increases in the percentages of NK cells in the peritoneal washes 3 days later (fig. S7), but B16-secMULT1 cells induced more potent *ex vivo* killing activity against NK-sensitive YAC-1 tumor cells (Fig. 2A). Similar results were obtained with RMA-secMULT1

cells (fig. S8A). Furthermore, higher percentages of peritoneal NK cells from mice injected with B16-secMULT1 cells produced IFN $\gamma$  after stimulation *ex vivo* with YAC-1 tumor cells (Fig. 2B) or immobilized antibodies against NK activating receptors (Fig. 2C, fig. S8B). To allow the recovery of intratumoral NK cells at early times after subcutaneous transfer, we implanted  $3\text{--}5 \times 10^5$  tumor cells mixed with matrigel. Seven days later, NK cells extracted from B16-secMULT1 tumors exhibited stronger IFN $\gamma$  responses after stimulation *ex vivo* (Fig. 2D). Therefore, soluble MULT1 stimulated NK cell functional capacities in both subcutaneous and peritoneal tumors.

Recombinant MULT1 (rMULT1) is similar in size to shed MULT1. When injected with B16 tumor cells (fig. S9A), rMULT1 resulted in partial tumor rejection (Fig. 2E, fig. S9B), and NK cells extracted from the tumors exhibited increased functional activity after stimulation *ex vivo* (Fig. 2F). The rMULT1 sample was devoid of endotoxin or other PAMPs that activate macrophages (fig. S9C). These data established that soluble MULT1 causes tumor rejection, likely by activating NK cells.

secMULT1 and shed MULT1 are monomeric (fig. S10A–C), and should not crosslink NKG2D, which is typically necessary for immune receptor activation. Indeed, monomeric rMULT1 failed to stimulate IFN- $\gamma$  production when incubated with peritoneal NK cells for 4 hours (fig. S11A). Soluble MULT1 may form a multivalent array *in vivo*, but preliminary staining analyses failed to detect such arrays. These data argue that soluble MULT1 stimulates NK cells by other mechanisms.

Target cells bearing membrane NKG2D ligands, including MULT1, caused downregulation of cell surface NKG2D, presumably by aggregating the receptor and triggering receptor endocytosis (8, 17) (Fig 3A). Tumor cells secreting secMULT1, in contrast, caused NKG2D upregulation on NK cells *in vivo* (Fig. 3A, 3B), without affecting an irrelevant receptor, DNAM-1 (Fig 3B). NKG2D upregulation occurred without increases in NKG2D mRNA (fig. S12) or intracellular protein. These findings suggested the following hypothesis (Fig. 3C): that untransformed host cells express membrane NKG2D ligands that persistently engage NK cells, cause NKG2D downregulation, and globally desensitize the NK cells as the tumors progress; and that soluble MULT1 enhances responsiveness and cell surface NKG2D expression by blocking these interactions.

Consistent with the hypothesis, host CD11b<sup>+</sup>F4/80<sup>+</sup> myeloid cells associated with either peritoneal or subcutaneous B16 or B16-secMULT1 tumors displayed the NKG2D ligand RAE-1 (but not MULT1) on the cell surface (Figure 3D, E). Monocytes in patients with several types of cancer also expressed NKG2D ligands (18). Tumors may cause an increase in RAE-1 expression by myeloid cells in the peritoneum (Fig. 3D) and possibly other sites (19). Hence, myeloid cells, and possibly other host cells, express NKG2D ligands *in vivo*. We further demonstrated that rMULT1 competitively blocks binding of RAE-1 $\epsilon$ -Fc fusion protein to NKG2D on NK cells (Fig. 3F), confirming a distinct prediction of the hypothesis.

To test whether RAE-1 expressed on endogenous cells caused NK cell inactivation, we employed the CRISPR/Cas9 method to disrupt both B6 strain RAE-1 genes, *Raet1d* and *Raet1e*. Peritoneal NK cells from *Raet1d*<sup>-/-</sup>*Raet1e*<sup>-/-</sup> mice exhibited significant increases in

membrane NKG2D expression as well as functional responses (Fig. 4A–C). Greater differences occurred when the mice were injected with irradiated B16 tumor cells, suggesting that greater NK desensitization and NKG2D downregulation occurs in the presence of tumors. The increase did not fully account for the effects of secMULT1 (Fig. 4A, 4B), suggesting that secMULT1 may also operate by other mechanisms. Notably, NK cells in *Raet1*-deficient mice exhibited greater responses to both NKG2D-dependent stimuli (e.g. to YAC-1 cells, Fig. 4B) and NKG2D-independent stimuli (e.g. to anti-NKp46, Fig. 4C), consistent with published reports that persistent stimulation by cells expressing NKG2D ligands results in a global desensitization of NK cells (17, 20). In mice injected with B16-secMULT1 tumor cells, smaller differences were observed, as predicted if secMULT1 blocks NKG2D interactions with RAE-1-expressing cells. Indeed, addition of rMULT1 to cultures of peritoneal wash cells, which contain NK cells and RAE-1+ myeloid cells, resulted in increased responses of NK cells to stimulation, when tested 8–20hrs later (fig. S11B, C). These data indicated that interactions of NK cells with RAE-1 molecules on non-tumor cells cause NKG2D downregulation and functional desensitization, and that this may be accentuated in tumor-bearing mice.

Our model further predicts that NKG2D receptor deficiency, or blocking with antibody, should have a similar effect as soluble MULT1. NK cells from NKG2D-deficient (*Klrk1*<sup>-/-</sup>) mice exhibited a modest increase in functional activity (fig. S13A), confirming recent findings (21, 22). A larger effect was evident in NKG2D-deficient NK cells on a *Rag2*<sup>-/-</sup> background (Fig. 4D). Similarly, i.p. injections of B6 mice with F(ab')<sub>2</sub> fragments of blocking NKG2D antibody resulted in enhanced functional responses ex vivo (Fig. 4E). Most remarkably, NKG2D-deficient *Rag2*<sup>-/-</sup> mice exhibited a strongly enhanced rejection response against B16 and B16-secMULT1 tumors, compared to the responses of *Rag2*<sup>-/-</sup> mice (Fig. 4F, G). Furthermore, incorporation of F(ab')<sub>2</sub> fragments of blocking NKG2D antibody into B16 tumors that were established in subcutaneous matrigel plugs resulted in partial tumor rejection and augmented responsiveness of NK cells within the residual tumors (fig. S13B, C). Thus, NKG2D deficiency, or blockade, results in enhanced NK cell responsiveness and tumor rejection. These data strongly support the proposed model (Fig. 3C).

The finding that NK cells persistently stimulated through NKG2D or other receptors are broadly desensitized is consistent with published data (20, 23) and may reflect a defect in MAPK/ERK signaling (23). Blocking or disabling NKG2D restores killing of B16 cells because NK cells use receptors distinct from NKG2D to target B16 cells. A more complex outcome should pertain with tumor cells that express membrane NKG2D ligands, because the NK cells, while more active, will be partly blocked in tumor cell recognition. Tumor cells often express multiple NKG2D ligands, suggesting that therapeutic efficacy may be maximized by blocking only the specific NKG2D ligands expressed by host cells, rather than blocking NKG2D altogether.

Our results are surprising as they show that soluble NKG2D ligands in vivo stimulate tumor rejection and increase membrane NKG2D, whereas the literature suggests they should suppress tumor rejection and decrease membrane NKG2D. It is notable, however, that NKG2D downregulation is frequently not observed in patients with soluble MICA/MICB

(6–9). Moreover, MULT1 and MICA/MICB ligands differ in a key respect: affinity. Soluble MULT1 is a high affinity ( $K_D \sim 10$  nM) monomeric ligand. Soluble MICA and MICB are low affinity ligands ( $K_D \sim 1$   $\mu$ M), which are present in patient sera at concentrations below 1 nM (4, 24), meaning that NKG2D occupancy is predicted to be extremely low. This consideration suggests that systemic effects of soluble MICA and MICB may be indirect, or that the active form of soluble MICA or MICB is actually a multimeric exosome form (25, 26), which can bind and crosslink the receptors despite a low affinity and low concentration. Binding and crosslinking are conditions known to cause modulation of other immune receptors from the cell surface (27). B16 cells secreting the low affinity MICA ligand, when injected i.p., failed to induce significant NKG2D upregulation or increased NK functional activity (fig. S14), in line with our expectations. In conclusion, the results identify an unexpected mechanism of immune activation and support efforts to evaluate the potential of soluble NKG2D ligands or antibodies that block NKG2D or its ligands for immunotherapy of cancer. Studies suggest that engagement of other NK activating receptors, such as NKp46, may also lead to NK cell desensitization, suggesting that multiple targets exist for amplifying NK function (28).

## Supplementary Material

Refer to Web version on PubMed Central for supplementary material.

## Acknowledgments

We thank H. Nolla and A. Valeros for help with cell sorting, C. Kang for targeting eggs for creating the *Raet1* knockout mice, Q. Yan for assistance with Biacore assays, and T. Trevino, L. Bai, S. Li for technical assistance. We thank Raulet Lab members and R. Vance for useful discussion and comments on the manuscript. The data presented in this manuscript are tabulated in the main paper and in the supplementary materials. David Raulet is an inventor on a patent (US 6821522) filed by UC Berkeley describing the use of soluble ligands for immunotherapy of cancer. WD was supported by a Cancer Research Institute postdoctoral fellowship. BG was supported by a National Science Foundation Graduate Research Fellowship and the Hirth Chair Graduate Fellowship of UC Berkeley. LW and AI were supported by Leukemia and Lymphoma Society Fellowships, and SL was supported by an NIH-IMSD grant. This work was supported by NIH grant R01 CA093678 to DHR.

## References

1. Raulet DH. Nat Rev Immunol. 2003; 3:781–790. [PubMed: 14523385]
2. Raulet DH, Gasser S, Gowen BG, Deng W, Jung H. Annu Rev Immunol. 2013; 31:413–441. [PubMed: 23298206]
3. Chitadze G, Bhat J, Lettau M, Janssen O, Kabelitz D. Scandinavian journal of immunology. 2013; 78:120–129. [PubMed: 23679194]
4. Groh V, Wu J, Yee C, Spies T. Nature. 2002; 419:734–738. [PubMed: 12384702]
5. Song H, Kim J, Cosman D, Choi I. Cell Immunol. 2006; 239:22–30. [PubMed: 16630603]
6. Salih HR, Goehlsdorf D, Steinle A. Hum Immunol. 2006; 67:188–195. [PubMed: 16698441]
7. Waldhauer I, Steinle A. Cancer Res. 2006; 66:2520–2526. [PubMed: 16510567]
8. Wiemann K, et al. J Immunol. 2005; 175:720–729. [PubMed: 16002667]
9. von Lilienfeld-Toal M, et al. Cancer Immunol Immunother. 2009
10. Guerra N, et al. Immunity. 2008; 28:571–580. [PubMed: 18394936]
11. Eagle RA, et al. PLoS One. 2009; 4:e4503. [PubMed: 19223974]
12. Xia M, et al. Circulation. 2011; 124:2933–2943. [PubMed: 22104546]
13. Carayannopoulos LN, Naidenko OV, Fremont DH, Yokoyama WM. J Immunol. 2002; 169:4079–4083. [PubMed: 12370332]

14. Nice TJ, Coscoy L, Raulet DH. *J Exp Med*. 2009; 206:287–298. [PubMed: 19171762]
15. Glas R, et al. *Journal of Experimental Medicine*. 2000; 191:129–138. [PubMed: 10620611]
16. Diefenbach A, Jensen ER, Jamieson AM, Raulet DH. *Nature*. 2001; 413:165–171. [PubMed: 11557981]
17. Oppenheim DE, et al. *Nat Immunol*. 2005; 6:928–937. [PubMed: 16116470]
18. Crane CA, et al. *Proc Natl Acad Sci U S A*. 2014; 111:12823–12828. [PubMed: 25136121]
19. Nausch N, Galani IE, Schlecker E, Cerwenka A. *Blood*. 2008
20. Coudert JD, Scarpellino L, Gros F, Vivier E, Held W. *Blood*. 2008; 111:3571–3578. [PubMed: 18198346]
21. Zafirova B, et al. *Immunity*. 2009
22. Sheppard S, et al. *Blood*. 2013; 121:5025–5033. [PubMed: 23649470]
23. Ardolino M, et al. *J Clin Invest*. 2014; 124:4781–4794. [PubMed: 25329698]
24. Marten A, von Lilienfeld-Toal M, Buchler MW, Schmidt J. *Int J Cancer*. 2006; 119:2359–2365. [PubMed: 16929491]
25. Clayton A, et al. *J Immunol*. 2008; 180:7249–7258. [PubMed: 18490724]
26. Ashiru O, et al. *Cancer Res*. 2010; 70:481–489. [PubMed: 20068167]
27. Taylor RB, Duffus WP, Raff MC, de Petris S. *Nature: New biology*. 1971; 233:225–229. [PubMed: 20480991]
28. Narni-Mancinelli E, et al. *Science*. 2012; 335:344–348. [PubMed: 22267813]



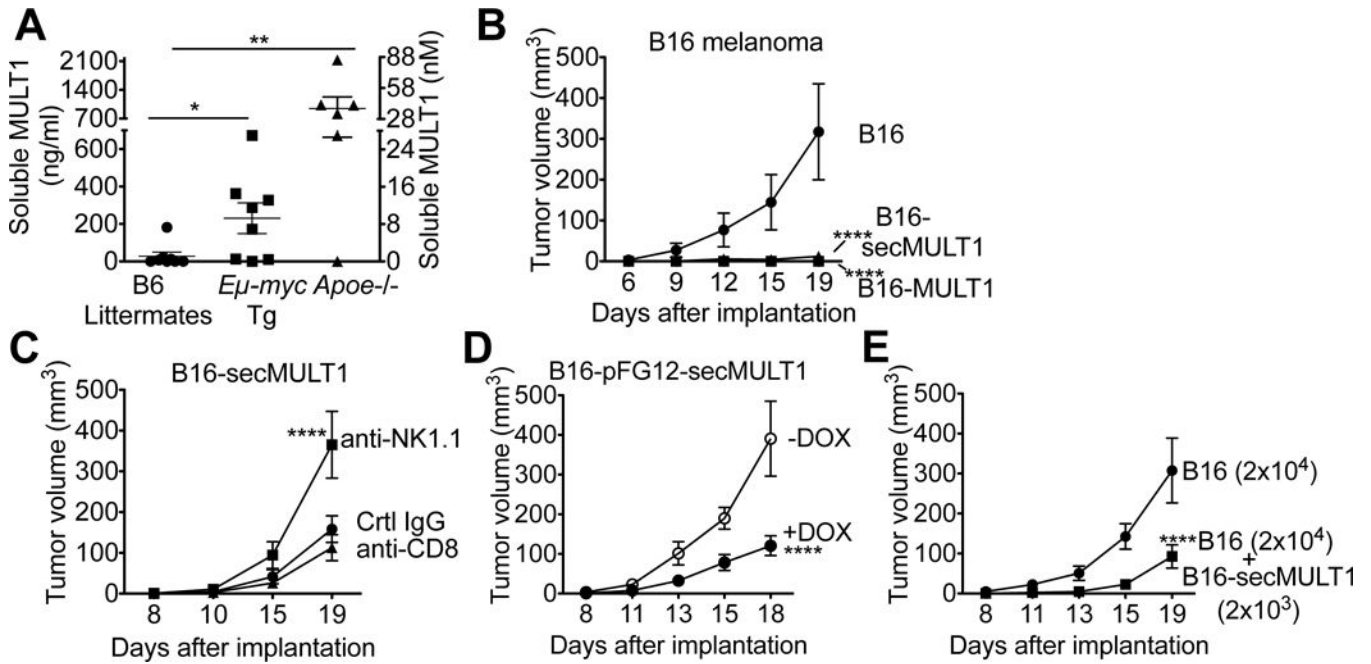


**Figure 1. NK cells promote the rejection of tumors that shed MULT1**

(A) ELISA detection of soluble MULT1 in sera from tumor bearing *Eμ-Myc* mice, nontransgenic littermates, and diseased *Apoe-/-* mice fed a Western diet (n=6–8). Each point represents a different mouse. (B) Comparison of growth of  $2 \times 10^4$  subcutaneously transferred B16 melanoma tumor cells transduced with secMULT1, full length MULT1 or empty vector, in WT B6 mice (n=4 mice). Rejection was usually partial but was complete in some animals in some experiments. (C) Subcutaneous growth of B16-secMULT1 tumors in B6 mice ( $2 \times 10^4$  cells were inoculated) treated with control IgG, NK1.1 antibody or CD8 antibody (n=13 mice). (D) After inoculation of  $2 \times 10^4$  B16 cells transduced with pFG12-secMULT1, mice were treated or not with doxycycline starting from the time of tumor implantation (n=6 mice). (E) Mice (n=6) received  $2 \times 10^4$  B16 cells alone, or  $2 \times 10^4$  B16 cells mixed with  $2 \times 10^3$  B16-secMULT1 cells. Panels show representative examples of 3 (panels B and E) or 2 (panel D) experiments performed, whereas panel C includes combined data from 3 experiments. Tumor volumes  $\pm$  SE are shown. Panel A was analyzed with a Mann-Whitney test, and panels B-E were analyzed by 2 way ANOVA with Bonferroni multiple comparison tests. \* $P < 0.05$ , \*\* $P < 0.01$ , \*\*\* $P < 0.001$  and \*\*\*\* $P < 0.0001$ .

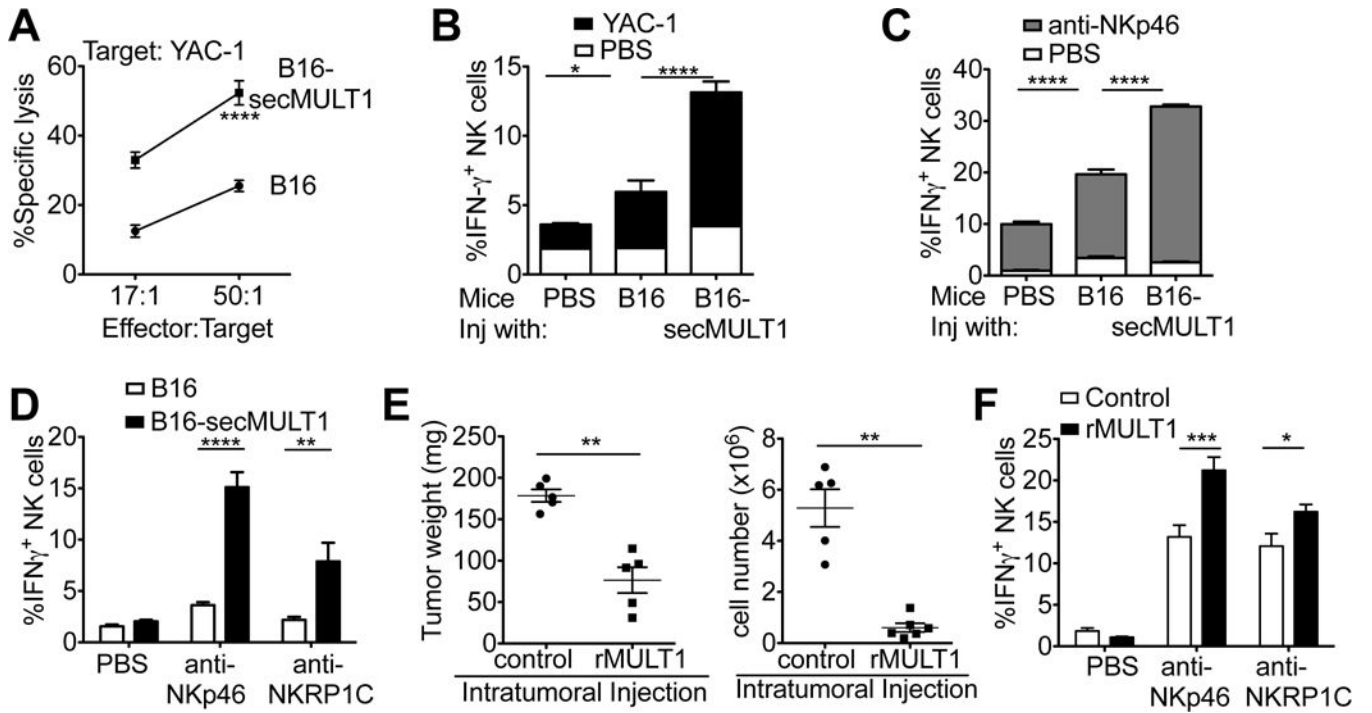


**Figure 2. Soluble MULT1 amplifies NK cell responses and causes tumor rejection**  
 (A–C) B6 mice were injected i.p. with  $5 \times 10^6$  irradiated B16 or B16-secMULT1 cells, or PBS. Peritoneal wash cells (pooled from 5 mice) were recovered three days later and tested for killing of YAC-1 target cells (A) or tested for intracellular IFN $\gamma$  after stimulation with YAC-1 cells (B) or immobilized NKp46 antibody (C); control responses to PBS are depicted by white segments of the bars. (D) B6 mice were injected subcutaneously with  $3\text{--}5 \times 10^5$  B16 or B16-secMULT1 cells in 100  $\mu$ l matrigel. The tumors were dissociated 7 days later, and gated NK cells from individual mice (n=5) were tested for responses to immobilized NKp46 or NKRP1C Abs. (E–F) Subcutaneous tumors were established with  $3\text{--}5 \times 10^5$  B16 cells in matrigel. The tumor cells in one group were mixed with 1  $\mu$ g of recombinant MULT1 (rMULT1). After 4 days, an additional 1  $\mu$ g of rMULT1 (or PBS for control mice) was injected into each matrigel/tumor for that group. On day 7, tumors were extracted, weighed (E), dissociated, and the tumor cells were counted (E). The immune cells within the tumors were stimulated with immobilized NKp46 and NKRP1C Abs, and the IFN $\gamma$  responses of gated NK cells were determined (F). Panels show representative examples of 2 (panel A) or 3 (panels B–F) experiments performed. Panels A–D and F were analyzed by 2-way ANOVA with Bonferroni multiple comparison tests, panel E was analyzed by Mann-Whitney test. \* $P < 0.05$ , \*\* $P < 0.01$ , \*\*\* $P < 0.001$  and \*\*\*\* $P < 0.0001$ .



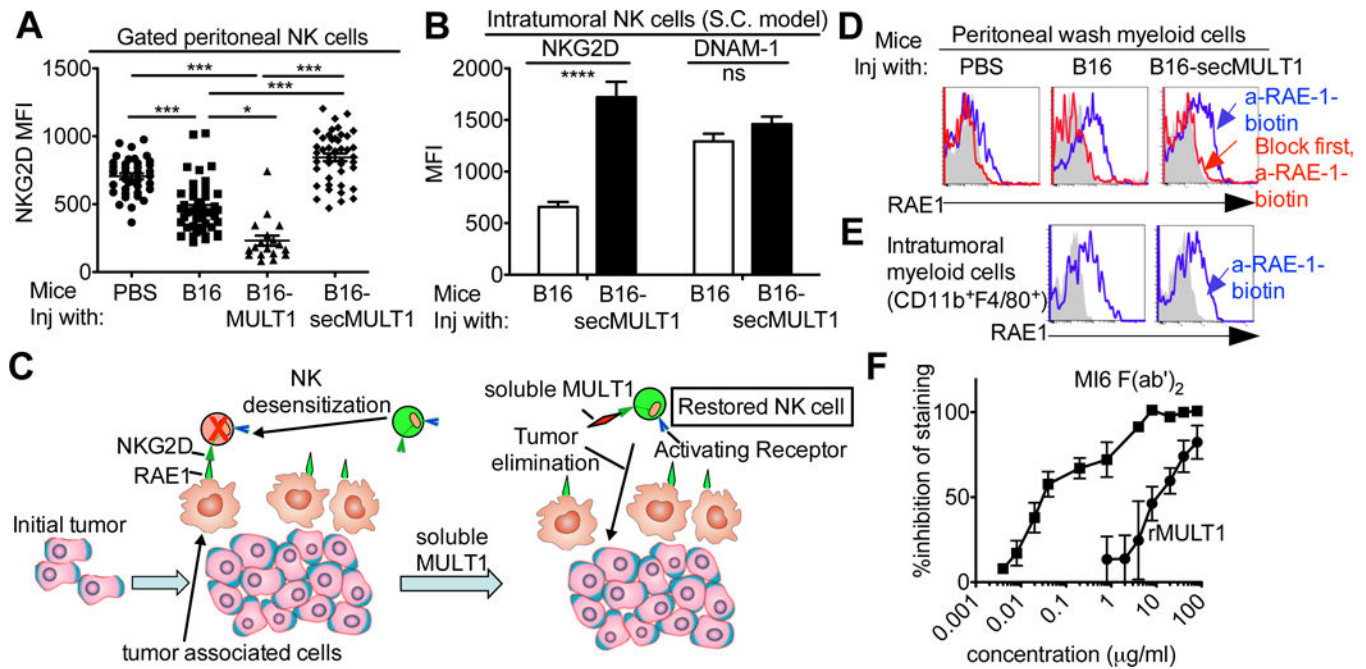


**Figure 3. Mechanisms of immune activation by soluble MULT1**

(A, B) Membrane NKG2D staining after exposure of NK cells to secMULT1 in intraperitoneal (A) or subcutaneous (B) tumors. (C) Model of secMULT1 action. Persistent NKG2D engagement by endogenous NKG2D ligand-expressing cells associated with the tumor desensitizes NK cells. Soluble MULT1 competitively blocks the NKG2D receptor, preventing NK cell desensitization and therefore augmenting tumor rejection mediated through distinct NK activating receptors. (D) Expression of NKG2D ligand RAE-1 by gated CD11b<sup>+</sup>F480<sup>+</sup> peritoneal myeloid cells in mice injected i.p. 3 days before with PBS or  $5 \times 10^6$  irradiated B16 or B16-secMULT1 tumor cells. Cells were stained with biotin-pan-RAE-1 Ab (blue). The staining was specific as it could be blocked by including an excess of unconjugated pan-RAE-1 antibody in the reaction (red). Grey shows isotype control staining. (E) Expression of RAE-1 by gated CD11b<sup>+</sup>F480<sup>+</sup> intratumoral myeloid cells in mice injected SC with  $2 \times 10^4$  B16 or B16-secMULT1 tumor cells 20 days before. (F) rMULT1 and NKG2D antibody (MI6 clone, in F(ab')<sub>2</sub> form) block RAE-1 binding to NKG2D on NK cells. The MFI of RAE1ε-Fc staining of NK cells was used to calculate % inhibition. Panel A is combined data from 14 experiments. Panels B, D–F show representative examples of 3 experiments performed. Panel A was analyzed by one-way ANOVA Kruskal-Wallis test, panel B was analyzed by 2-way ANOVA with Bonferroni multiple comparison tests, ns indicates  $P > 0.05$ , \* $P < 0.05$ , and \*\*\* $P < 0.001$ .

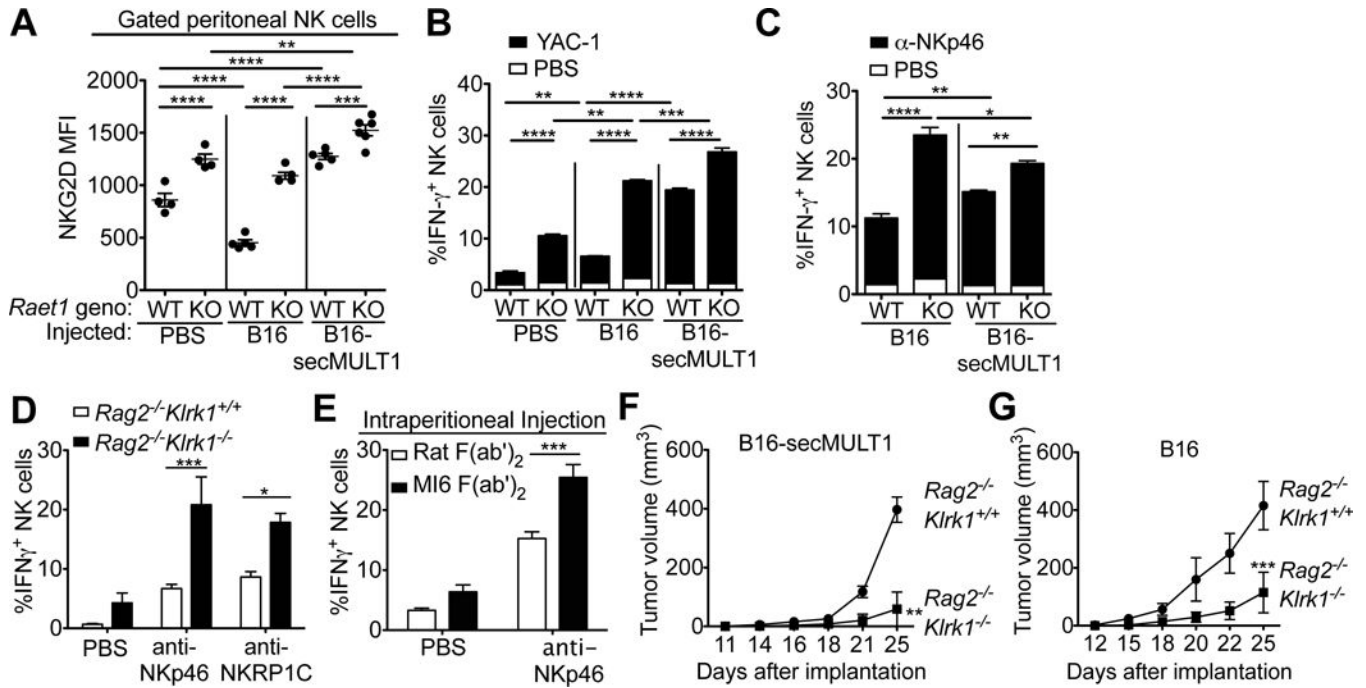


**Figure 4. Augmented NK cell responses in RAE-1-deficient and NKG2D-deficient mice** (A–C) Peritoneal NK cells from *Raet1d*<sup>-/-</sup>*Raet1e*<sup>-/-</sup> mice (KO) exhibited increased amounts of cell surface NKG2D (A) and increased functional responses ex vivo to YAC-1 tumor cells (B) or NKp46 antibody stimulation (C); control responses to PBS are depicted by white segments of the bars. The effects were larger when the mice were injected 3 days earlier with irradiated B16 tumor cells, but smaller when they were injected with B16-secMULT1 tumor cells. (D) NKG2D-deficient (*Klrk1*<sup>-/-</sup>) NK cells exhibited increased functional activity. Splenic NK cells from *Rag2*<sup>-/-</sup> and *Rag2*<sup>-/-</sup> *Klrk1*<sup>-/-</sup> mice were stimulated ex vivo with immobilized NKp46 or NKRP1C Abs, and the IFN- $\gamma$  responses of gated NK cells were determined. (E) B6 mice were injected i.p. with 50  $\mu$ g MI6 (anti-NKG2D) F(ab')<sub>2</sub> or F(ab')<sub>2</sub> of rat IgG on days 0, 3 and 6. On Day 8, peritoneal NK cells were stimulated ex vivo with immobilized NKp46 Abs, and the IFN $\gamma$  responses of gated NK cells were determined. (F, G) Increased tumor rejection responses in NKG2D-deficient mice. Growth of B16-secMULT1 (F) or B16 (G) tumor cells in *Rag2*<sup>-/-</sup> or *Rag2*<sup>-/-</sup>*Klrk1*<sup>-/-</sup> mice (n=5). Panels F and G are from separate experiments. Separate, direct comparisons showed retarded growth of B16-secMULT1 vs B16 tumors in *Rag2*<sup>-/-</sup> mice. All experiments show representative examples of 3 experiments performed. Tumor volumes  $\pm$  SE are shown. Figure 4A–G were analyzed by 2-way ANOVA with Bonferroni multiple comparison tests. \* $P < 0.05$ , \*\* $P < 0.01$ , \*\*\* $P < 0.001$  and \*\*\*\* $P < 0.0001$ .